

Automatic interpretation of magnetic data using Euler deconvolution with nonlinear background

**Pawan Dewangan, T. Ramprasad, M. V. Ramana, M. Desa, and B.
Shailaja**

**Geological Oceanography, National
Institute of Oceanography, Dona Paula, Goa-403004, India**

(May 5, 2007)

ABSTRACT

The voluminous gravity and magnetic datasets demand automatic interpretation techniques like Naudy, Euler and Werner deconvolution. Of these techniques, the Euler deconvolution has become a popular choice because the method assumes no particular geological model. However, the conventional approach to solving Euler equation requires tentative values of the structural index preventing it from being fully automatic and assumes a constant background that can be easily violated if the singular points are close to each other. We propose a possible solution to these problems by simultaneously estimating the source location, depth and structural index assuming nonlinear background. The Euler equation is solved in a nonlinear fashion using optimization technique like conjugate gradient. This technique is applied to a published synthetic dataset where the magnetic anomalies were modeled for a complex assemblage of simple magnetic bodies. The results for close by singular points are superior to those obtained by assuming linear background. We also applied the technique to a magnetic dataset collected along the western continental margin of India. The results are in agreement with the regional magnetic interpretation and the bathymetric expressions.

INTRODUCTION

The advancement in acquisition technique leads to routine collection of magnetic and gravity datasets (HARTMAN *et al.*, 1971; REID *et al.*, 1990). The large data volume demands automatic techniques like Naudy (NAUDY, 1971), Euler (THOMPSON, 1982) and Werner deconvolution (WERNER, 1953) for the interpretation of magnetic and gravity anomalies. Euler deconvolution has emerged as a powerful technique for estimating the depth and the geometry of the buried magnetic sources (THOMPSON, 1982; REID *et al.*, 1990). This technique has become popular because it requires no a priori information about the source magnetization and it assumes no particular geological model. THOMPSON (1982) developed this technique for profile data while REID *et al.* (1990) extended it for gridded data.

However, direct application of Euler deconvolution to magnetic data leads to unreliable and erratic results because the magnetic field of an isolated body is seldom recorded in the field and is generally perturbed by the magnetic field of nearby bodies. Several authors (THOMPSON, 1982; REID *et al.*, 1990; BARBOSA *et al.*, 1999) have addressed this issue by assuming a constant regional background. This assumption introduces nonlinearity in the Euler equation. However, it can still be solved in a linear fashion by assuming tentative values of the structural index. The structural index (SI) can be determined by observing the clustering of solutions for different SI values. For a particular feature, the correct SI yields a tight cluster. REID *et al.* (1990) showed with the help of synthetic examples that if an index is underestimated depth will also be underestimated and vice versa. This method of estimating depths by varying the SI has become an accepted norm in geophysical literature (BARBOSA *et al.*, 1999). The use of tentative values of SI has prevented the technique from being fully automatic. The method has become subjective and time consuming as the interpreter has to judge the quality of clustering for different features as the index is varied.

An alternative approach is to estimate the source location, depth and SI simultaneously assuming constant background (HSU, 2002; GEROVSKA *et al.*, 2005). This approach is fully automatic and yields reliable estimates if the background field can be adequately represented as a constant. However, the assumption of constant background is too simplistic if the singular points are located close to each other. The above problem was addressed by STAVREV (1997) by proposing an algorithm for linearizing Euler equation with unprescribed structural index and linear background. The algorithm works on the principle of Differential Similarity Transform (DST). GEROVSKA and ARAÚZO-BRAVO (2003) demonstrated the technique on a real and a synthetic dataset, modeled for a complex assemblage of simple magnetic bodies. They showed that simultaneous estimation of both the source coordinate and SI is possible using linear inversion assuming linear background. In the synthetic example, however, some singular points show significant error in depth and SI due to the nonlinearity of the background field.

In this paper, we propose to estimate both the source location and SI using Euler deconvolution assuming nonlinear background. We approximate the regional field using a rational function in which both the numerator and denominator are linear. The Euler equation is solved in nonlinear fashion to estimate the source location, depth, SI and the coefficients of rational function. We apply the method to the same synthetic dataset as used by GEROVSKA and ARAÚZO-BRAVO (2003) and show that the estimates of depth and SI for close by singular points have improved. The estimates of other singular points remain unaltered.

The most widely used norm to eliminate the spray of solutions is based on the standard deviation of the depth (THOMPSON, 1982), which can be estimated from the least-square solution. Since, such an acceptance criteria is not possible for nonlinear inversion, we eliminated the erroneous solutions by using the criteria suggested by SILVA and BARBOSA (2003). They suggested that the precision of depth and SI can be improved if the computation is confined to the flat area of horizontal source location.

Using synthetic examples, we show that such an acceptance criteria is equivalent to that suggested by THOMPSON (1982). Finally, we applied the proposed algorithm to marine magnetic data along the western continental margin of India. The resultant fracture network agrees with the regional structural trends (SUBRAHMANYAM *et al.*, 1995) and shows positive correlation with bathymetry.

THEORY

Euler deconvolution is based on the Euler homogeneity equation which could be written in the form,

$$(x - x_0)\frac{\partial T}{\partial x} + (y - y_0)\frac{\partial T}{\partial y} + (z - z_0)\frac{\partial T}{\partial z} + \eta T = 0. \quad (1)$$

The total magnetic field anomaly (T) is due to the magnetic source located at (x_0, y_0, z_0) ; η is the SI related to the simple source geometry. Equation (1) can be solved in a least-square fashion to obtain the source coordinates and its geometry. However, direct application of equation (1) to the observed data is not useful because the absolute value of the anomalous field (T) is rarely known. Equation (1) does not account for the regional or background magnetic field due to nearby sources, as a result the exact solution is unreliable and erratic (THOMPSON, 1982).

In general, the unknown regional field (B) can be approximated using Taylor series as,

$$B(x, y) = B_0 + x \frac{\partial B}{\partial x} + y \frac{\partial B}{\partial y} + O(2), \quad (2)$$

where B_0 is the constant background at the center of the specified window and $O(2)$ represents higher-order terms in the Taylor series expansion. The anomalous field (T) can now be expressed as the difference between the observed (F) and regional (B) fields,

$$T = F - B. \quad (3)$$

The modified Euler equation is obtained by substituting T into equation (1),

$$\mathcal{F} \equiv (x - x_0) \frac{\partial(F - B)}{\partial x} + (y - y_0) \frac{\partial(F - B)}{\partial y} + (z - z_0) \frac{\partial(F - B)}{\partial z} + \eta(F - B) = 0. \quad (4)$$

For isolated or well separated bodies, Euler equation gives acceptable solution by considering the leading-order term in Taylor series expansion or constant background (THOMPSON, 1982; REID *et al.*, 1990). In such a scenario, Euler equation becomes nonlinear and is solved linearly by assuming tentative values of the SI (THOMPSON, 1982; REID *et al.*, 1990). The Euler equation can also be solved linearly assuming constant background (HSU, 2002; GEROVSKA *et al.*, 2005). For close by singular points, the assumption of constant background might be too simplistic and needs linear term of Taylor series expansion. This problem was addressed by STAVREV (1997) and GEROVSKA and ARAÚZO-BRAVO (2003) using Differential Similarity Transform (DST). They showed that the Euler equation can be solved linearly for both the source location and SI assuming linear background. If the singular points are located very close to each other, such as the multiple fracture sets, sill etc, then the assumption of linear background breaks down and demands higher-order terms of Taylor series expansion [equation (2)] for unbiased solution.

We explore the possibilities of using nonlinear background in Euler equation. The obvious choice is to use the second-order terms of the Taylor series expansion [equation (2)] but we prefer to use the rational approximation in which the infinite Taylor series expansion is approximated by two polynomials, one in numerator and other in denominator. The rational function is chosen because the error involved in the calculation using n terms of the rational approximation is less than or equal to the error using $2n$ terms of Taylor series (KOPAL, 1961) and the rational approximation forms an infinite series which allows one to approximate a larger class of functions using fewer terms than a series. In fact, the Taylor series expansion is a special case of the rational approximation where the denominator is 1. We prefer to use a first-order

term in both numerator and denominator because the maximum accuracy in rational approximation is achieved when the powers in the polynomials of numerator and denominator are the same (KOPAL, 1961). So, the background can be approximated using a rational function as,

$$B(x, y) = \frac{B_0 + ax + by}{1 + cx + dy}, \quad (5)$$

where $B_0, a, b, c,$ and d are the unknown coefficients. Substituting equation (5) into (4) yields the nonlinear Euler equation. This equation can be solved for the source location, depth, SI and the coefficients of rational function using nonlinear optimization technique like precondition conjugate gradient (COLEMAN and LI, 1996). Another advantage of this approach is that the apriori information like the upper and lower bounds for depth and SI (0 – 3) can be easily incorporated into the inversion algorithm thereby eliminating unrealistic solutions. We tested the proposed algorithm using synthetic and real data examples.

METHODOLOGY

The basic framework for applying Euler deconvolution to a gridded magnetic data is given by REID *et al.* (1990). They showed that pole reduction prior to Euler deconvolution is unnecessary as the source positions can be accurately reproduced without reducing the data to the poles. Here we follow the same approach and prefer to work on the original data. The Euler deconvolution needs the total magnetic field anomaly and its spatial derivatives in $x, y,$ and z directions. For the calculation of horizontal spatial derivatives, the field is approximated with bicubic splines to minimize the amplification of noise during the differentiation. Usually, the vertical derivative is not measured in the field and it requires special attention. The vertical derivative is obtained in the frequency domain following NABHIGIAN (1984). To remove the edge effects, half a cosine function is used to extend the grid by 10% in the x

and y direction before the calculation of vertical derivative. The extended area of the obtained derivative grid is then clipped back to the initial grid size.

After calculating spatial derivatives for the whole grid, a small convolution window is chosen for the application of Euler deconvolution. Conventional wisdom is to make the convolution window width not less than half the maximum expected depth to the source (FITZGERALD *et al.*, 2004). The required quantities for Euler deconvolution are extracted for the convolution window and Euler equation is solved nonlinearly assuming nonlinear background. A nonlinear optimization technique like precondition conjugate gradient (COLEMAN and LI, 1996) is used to minimize the error function $\|\mathcal{F}\|$ [equation 4] for all data points within the convolution window. To start the inversion, an initial guess for the source location, depth, SI and the coefficients of rational function is required. The initial guess for the source location is assumed to be the center of the specified window, the coefficients of rational approximation are set to zero and the values of depth and SI are arbitrarily chosen. We observe that an initial model with incorrect depth and SI is more likely to converge to local minima than to the global minimum. The choice of initial guess for other parameters is not critical in deciding the convergence of a starting model to the global minimum. Therefore, an initial model with depth and SI values close to the correct ones is required to find global minimum and for faster convergence. This can be achieved by running the inversion with hundreds of starting models adequately sampling the model space of depth and SI. For each initial model, the depth and SI values are obtained randomly from a uniform distribution so that its model space is evenly sampled. The upper and lower bounds of depth and SI are decided by the user based on the existing geological information. The ranges of depth and SI values should be wide enough to encompass all geological bodies. The choice of other parameters remains unchanged. The nonlinear optimization is performed for each of the starting models to obtain a plausible solution and the residual error is calculated as a squared 2-norm at the solution to measure the misfit between the observed and calculated

data points. A large number of plausible models are obtained by choosing hundreds of starting models. Out of all possible models, the solution which has the least residual error is selected as the final solution. By carefully choosing the bounds of the starting model, the user can not only eliminate unreasonable depths but also limit the search of magnetic sources based on its SI.

The convolution window is scrolled across the grid to obtain the estimate of the source location, depth and SI for different features. In order to clean the spray of solutions, we decided to use the criteria suggested by SILVA and BARBOSA (2003). The flat surface of the horizontal source locations (x_0, y_0) represents consistent estimates and should be used to identify good solutions. The flatness can be mathematically defined as,

$$AccCri \equiv \sqrt{\left(\frac{\partial x_0}{\partial x}\right)^2 + \left(\frac{\partial x_0}{\partial y}\right)^2 + \left(\frac{\partial y_0}{\partial x}\right)^2 + \left(\frac{\partial y_0}{\partial y}\right)^2} < \tau_0 \quad (6)$$

All solutions below a threshold value (τ_0) , defined by the user, are acceptable. The good solutions are interpreted as distinct geometrical bodies with certain depth based on its SI (THOMPSON, 1982).

Synthetic example

We tested the proposed algorithm on a published dataset of a complex assemblage of five simple bodies (GEROVSKA and ARAÚZO-BRAVO, 2003). The model consists of five causative bodies with ten singular points: two spheres (isometric bodies), one S1 at a depth of 3 km and another one S5 at 2 km; one sheet body (sill) S2, a dyke infinite in depth extent S3 and a horizontal rod S4. The magnetization and the direction of the ambient field remains the same as mentioned in the original paper. The total magnetic field anomaly for the five simple bodies is shown in Figure 1. The details of all the singular points arranged with respect to their identification number are given in Table 1. Applying Euler deconvolution with linear background to the

gridded synthetic data, GEROVSKA and ARAÚZO-BRAVO (2003) obtained the estimates of source locations (\hat{x}_0, \hat{y}_0) , depth (\hat{z}_0) and SI $(\hat{\eta})$ as shown in Table 1. The details of the parameter required for Euler deconvolution can be found in GEROVSKA and ARAÚZO-BRAVO (2003). In general, the means of the estimated values show good agreement with the correct parameters (Table 1). However, the depth and SI of singular points *three* and *four* of the horizontal sill are biased due to the strong interference of nearby singular points (2-5, Fig. 1). The small number of solutions for the singular point *nine* of the horizontal rod and large bounds in SI for the singular point *seven* of the dyke and *nine* and *ten* of the horizontal rod can be attributed to the presence of nonlinear background which was not accounted in the algorithm of STAVREV (1997).

We applied the proposed Euler deconvolution with nonlinear background to the same synthetic dataset. The dataset was freely available along with the matlab codes of GEROVSKA and ARAÚZO-BRAVO (2003). The magnetic data was sampled at a regular interval of 0.25 km. The convolution window was set to be 11×11 points (2.5×2.5 km). The lower and upper bounds for the depth and SI were assumed to be 0–5 and 0–3.5 respectively. Let us evaluate the algorithm's performance for the singular point of the sphere S1 (column index *six*) by running the inversion with approximately 5000 starting models. Each starting model was optimized to obtain a plausible solution and the residual error is calculated as a squared 2-norm at the solution to measure the misfit between the observed and calculated data points. Since the problem of local minima is associated with incorrect depth and SI values, we estimated a quantity D_i to measure the closeness of starting model to the true solution as,

$$D_i = \sqrt{(\text{depth}_i - \text{depth}_t)^2 + (\text{SI}_i - \text{SI}_t)^2}, \quad (7)$$

where the subscripts i and t represent the initial guess and the true value, respectively. In a similar fashion, the quantity D_t is estimated to measure the closeness of plausible solution to the true solution. The crossplot between the quantities D_i and

D_t evaluates the performance of the algorithm as shown in Fig. 2a. In general, the performance of the algorithm depends on the closeness of the starting model to the true solution. If the starting model is close to the true solution (zone 1 in Fig. 2a) the inversion converges to global minimum and the true solution is obtained. In zone 2, the probability that the starting model will converge to the true solution increases as the starting model approaches the true solution. The models that are far from the true solution (zone 3) fails to converge to global minimum. Out of all possible solutions, the best solution is the one which has the least residual error as shown in Fig. 2b. These conclusions remain valid for other singular points.

The problem of local minima was overcome by executing the code for hundred starting models with depth and SI values assigned randomly between the upper and lower bounds. The estimates of source location, depth and SI are obtained in a grid and the spray of solutions was eliminated by applying the acceptance criteria as discussed above. The tolerance limit was chosen in such a way that the number of solutions for the singular points (2-5) remain the same as in Table 1. For comparison, we adopted the same clustering approach and used the matlab codes of GEROVSKA and ARAÚZO-BRAVO (2003) to calculate the mean and uncertainty of the estimated quantities and the result is summarized in Table 2.

The isolated and strong anomalous bodies like S1 and S5 with singular points *six* and *one* show little or no difference in the estimated parameters. For close by singular points like *nine* of horizontal rod, the number of solutions has increased and the estimates of depth and SI have improved. For singular points like 2-5 of horizontal sill and 7-8 of dyke, the estimates of depth and SI are more close to the correct ones as shown in Table 1 and 2. In some cases like singular point *ten* of horizontal rod, the number of solutions is reduced but are tightly bound as compared to the result of linear inversion (Table 1). From the results of Euler deconvolution with linear and nonlinear background (Tables 1 and 2), we conclude that the estimate of close by singular points improves due to proper treatment of regional field in Euler equation.

For isolated and strong anomalies, the assumption of linear/constant background is valid and the results are equivalent.

FIELD DATA EXAMPLE

We applied the proposed algorithm to the total magnetic field anomaly from the Arabian Sea along the western continental margin of India (Fig. 3). The study area lies to the north of Chagos-Laccadive Ridge system. The magnetic field anomaly is predominantly due to Precambrian basement faults. The magnetic data was collected along several profiles oriented in NNW-SSE direction. The data are sampled at roughly 50 m along the profile direction, the distance between the profiles being approximately 3.7 km. A high cut filter was applied in the wavenumber domain before the calculation of spatial derivatives to enhance the signal-to-noise ratio. The partial derivative in the vertical direction was obtained by extending the field grid before the calculation. The convolution window was chosen to be 100×2 grid points (5×7.4 km) which is of the order of expected depth in the region. The minimum water depth in this region is 2.6 km which provides good a priori information for the lower bound. The upper bound is arbitrarily chosen to be 8 km, the maximum basement depth expected in this region. The SI is assumed to vary between 0 and 3 encompassing all plausible geological bodies. To overcome the problem of local minima, the code was executed using hundred starting models with depth and SI values assigned randomly between the upper and lower bounds. The estimates of source location, depth, SI and the coefficients of rational approximation are obtained by minimizing the error function using nonlinear optimization technique of COLEMAN and LI (1996).

The spray of solutions is cleaned by applying the acceptance criteria as discussed in this paper. The histogram plot of SI (Fig. 4) shows the absence of high SI bodies like sphere, cylinder, rod etc from the observed data. Most of the SI varies between 0.2-

0.5 suggesting that the magnetic anomaly is predominantly due to basement faults. WILLIAMS *et al.*, 2003 obtained similar range of SI for a synthetic example of faulted basement model. Approximately 2700 estimates of source location are plotted on top of the magnetic anomaly (Fig. 3) and the depth values are color coded. Figure 3 shows two sets of orthogonal fractures, predominantly oriented in the NW-SE and NE-SW directions. The orientation of the orthogonal fracture set agrees with the orientation obtained from regional magnetic interpretation (SUBRAHMANYAM *et al.*, 1995). In the southern region, the depth of the Precambrian basement derived from the faults is less than that in the northern region. Furthermore, intense fracturing is observed in the center of the grid. When we overlay the solutions of Euler deconvolution on the bathymetry contours (Fig. 5), it helps in explaining the depth of the basement in relation to water depth. In the southern region, the water depth is shallow compared to that of the northern region suggesting that the sediment thickness is uniform (1-1.5 km), which is reasonable as the sedimentation rate is expected to be a constant in deep oceanic environment. The constant sedimentation rate suggests that the feature observed in bathymetry must be related to Precambrian basement tectonics, which in turn is responsible for the magnetic anomaly. The intense fracturing at the center of the grid creates sharp basement rise as observed in the bathymetry. Thus, the fault network and depths estimated from the Euler deconvolution are in agreement with the bathymetric expressions and the structural trends obtained from the regional magnetic interpretation.

CONCLUSIONS

The improper treatment of regional background in the Euler equation often leads to erroneous results. Several authors have addressed this issue by assuming a constant background field which is valid for strong anomalies and well separated magnetic sources. The estimates of source location, depth and SI can be improved by assuming

a linear background and solving Euler equation in a linear fashion using Differential Similarity Transform. If the singular points are located very close to each other like multiple fracture sets, sill and closely spaced dyke then the assumption of linear background also breaks down and demands higher order fluctuation in the background field. We solved Euler equation in a nonlinear fashion assuming nonlinear background and showed on a published synthetic dataset that the estimate of depth and SI improves for close by singular points. For isolated or strong anomalies, the results are equivalent suggesting that the algorithm does not degrade by including redundant parameters. Another advantage of this technique is that the apriori information about the bounds of depth and SI can be easily incorporated into the inversion algorithm. As with any other nonlinear inversion, the proposed algorithm also suffers from the problem of local minima which can be avoided by running the inversion with a large number of starting models.

We applied the algorithm on a magnetic dataset obtained in the Arabian Sea along the western continental margin of India. The solutions of Euler deconvolution suggest that the magnetic anomalies are predominantly due to basement faulting and their orientation is consistent with that obtained from regional magnetic interpretation. Overlaying the solution on the bathymetry contours suggests that the sedimentation rate in this region is constant and the bathymetric expressions like the sharp basement rise in the center of the study region is governed by Precambrian basement tectonics.

ACKNOWLEDGMENTS

The authors wish to thank the Director, National Institute of Oceanography (NIO) for giving permission to publish this paper. The authors thank the anonymous reviewer for its invaluable comments and suggestions. This is NIO contribution no. xxxx.

REFERENCES

- Barbosa, V.C.F., Silva, J.B.C., and Medeiros, W.E. (1999), *Stability analysis and improvement of structural index estimation in Euler deconvolution*, Geophys. *64*, 48-60.
- Coleman, T.F. and Y. Li. (1996), *An interior, trust region approach for nonlinear minimization subject to bounds*, SIAM J. on Optimization *6*, 418-445.
- FitzGerald D., Reid A., and McInerney, P. (2004), *New discrimination techniques for Euler deconvolution*, Computers and Geosciences *30*, 461–469.
- Gerovska, D. and Araúzo-Bravo, M.J. (2003), *Automatic interpretation of magnetic data based on Euler deconvolution with unprescribed structural index*, Computers and Geosciences *29*, 949–960.
- Gerovska, D., Stavrev, Y., and Arauzo-Bravo, M.J. (2005), *Finite-difference Euler deconvolution algorithm applied to the interpretation of magnetic data from northern Bulgaria*, Pure App. Geophys. *162*, 591-608.
- Hartman, R.R., Teskey, D. J., and Friedberg, J.L. (1971), *A system for rapid digital aeromagnetic interpretation*, Geophys. *36*, 891–918.
- Hsu, S. K. (2002), *Imaging magnetic sources using Euler's equation*, Geophys. Prosp. *50*, 15-25.
- Kopal, Z. (1961), *Numerical analysis* (Chapman and Hall Ltd., London), pp. 551–553.
- Nabighian, M. N. (1984), *Towards a three-dimensional automatic interpretation of potential field data via generalized Hilbert transforms: Fundamental relations*, Geophys. *49*, 780–786.

- Naudy, H. (1971), *Automatic determination of depth on aeromagnetic profiles*, Geophys. *36*, 717–722.
- Reid, A.B., Allsop, J.M., Granser, H., Millet, A. J., and Somerton, I. W. (1990), *Magnetic interpretation in three dimensions using Euler deconvolution*, Geophys. *55*, 80–91.
- Silva, J.B.C. and Barbosa, V.C.F. (2003), *3D Euler deconvolution: Theoretical basis for automatically selecting good solutions*, Geophys. *68*, 1962–1968.
- Stavrev, P.Y. (1997), *Euler deconvolution using differential similarity transformations of gravity or magnetic anomalies*, Geophys. Prosp. *45*, 207-246.
- Subrahmanyam, V., Gopala Rao, D., Ramana, M. V., Krishna, K. S., Murty, G. P. S., and Gangadhara Rao, M. (1995), *Structure and tectonics of the southwestern continental margins of India*, Tectonophys. *249*, 267–282.
- Werner, S. (1953), *Interpretation of magnetic anomalies at sheet-like bodies*, Sver. Geol. Undersok., ser. C. C. Arsbok. , no. 06.
- Williams, S., Fairhead, J. D., and Flanagan, G. (2003), *Grid based Euler deconvolution: Completing the circle with ‘2D constrained Euler’*, SEG Technical Program Expanded Abstracts *22*, 576–579.
- Thompson, D. T. (1982), *EULDPH: A new technique for making computer-assisted depth estimates from magnetic data*, Geophys. *47*, 31–37.

TABLES

<i>index</i>	n_{sol}	$x_0 (km)$	$\hat{x}_0 (km)$	$y_0 (km)$	$\hat{y}_0 (km)$	$z_0 (km)$	$\hat{z}_0 (km)$	η	$\hat{\eta}$
1	82	10	9.9 ± 0.11	10	9.97 ± 0.03	2	1.92 ± 0.08	3	2.77 ± 0.19
2	10	25	24.97 ± 0.03	10.5	10.38 ± 0.01	1	1.08 ± 0.02	1	1.34 ± 0.04
3	24	27	27.11 ± 0.05	10.5	10.33 ± 0.04	1	0.71 ± 0.06	1	0.21 ± 0.13
4	25	27	27.12 ± 0.03	13.5	13.65 ± 0.04	1	0.72 ± 0.05	1	0.24 ± 0.13
5	23	25	24.86 ± 0.14	13.5	13.63 ± 0.03	1	0.91 ± 0.1	1	0.85 ± 0.32
6	170	17.5	17.49 ± 0.08	17.5	17.46 ± 0.07	3	2.95 ± 0.08	3	2.91 ± 0.15
7	343	22.5	22.6 ± 0.26	19	18.87 ± 0.92	1	0.81 ± 0.12	1	0.88 ± 0.64
8	335	22.5	22.51 ± 0.11	31	31.25 ± 0.26	1	0.83 ± 0.06	1	1.06 ± 0.25
9	30	15.25	15.34 ± 0.33	25	25.06 ± 0.43	1.5	1.45 ± 0.2	2	1.84 ± 0.83
10	542	8	7.76 ± 0.45	25	25.14 ± 0.53	1.5	1.54 ± 0.11	2	1.83 ± 0.51

TABLE 1. Estimated (denoted with a hat) and true coordinates of singular points and their respective structural indices for 5 bodies example after Gerovska and Arauzo-Bravo (2003). Column *index* denotes the identity number of the singular points and column *nsol* shows obtained number of solutions for one singular point.

<i>index</i>	<i>n_{sol}</i>	<i>x</i> ₀ (km)	<i>x̂</i> ₀ (km)	<i>y</i> ₀ (km)	<i>ŷ</i> ₀ (km)	<i>z</i> ₀ (km)	<i>ẑ</i> ₀ (km)	<i>η</i>	<i>η̂</i>
1	251	10	9.98 ± 0.06	10	10.00 ± 0.06	2	1.97 ± 0.13	3	2.95 ± 0.31
2	31	25	24.97 ± 0.07	10.5	10.39 ± 0.05	1	1.05 ± 0.10	1	1.24 ± 0.28
3	28	27	27.07 ± 0.07	10.5	10.43 ± 0.05	1	0.98 ± 0.20	1	1.06 ± 0.68
4	23	27	27.11 ± 0.12	13.5	13.55 ± 0.18	1	0.93 ± 0.18	1	0.93 ± 0.49
5	27	25	24.95 ± 0.08	13.5	13.63 ± 0.05	1	1.04 ± 0.05	1	1.17 ± 0.18
6	288	17.5	17.49 ± 0.08	17.5	17.47 ± 0.11	3	3.00 ± 0.10	3	2.99 ± 0.21
7	144	22.5	22.52 ± 0.06	19	18.69 ± 0.17	1	0.85 ± 0.08	1	1.10 ± 0.24
8	176	22.5	22.51 ± 0.03	31	31.26 ± 0.11	1	0.86 ± 0.04	1	1.17 ± 0.11
9	147	15.25	15.37 ± 0.06	25	24.99 ± 0.04	1.5	1.51 ± 0.06	2	2.02 ± 0.17
10	297	8	7.87 ± 0.10	25	25.01 ± 0.12	1.5	1.52 ± 0.07	2	1.98 ± 0.27

TABLE 2. Same as Table 1 but the estimates of source locations, depths and structural indices is obtained by applying Euler deconvolution with nonlinear background.

FIGURES

FIG. 1. Total magnetic field anomaly in nT for five simple bodies (after GEROVSKA and ARAÚZO-BRAVO, 2003); S1 and S5 are sphere, S2 is sill body, S3 is a dyke of infinite depth extent, and S4 is a horizontal rod. Each of the singular point is denoted by a circle with a unique number assigned to it.

FIG. 2. The performance of the algorithm is evaluated by crossplotting the quantities D_i and D_t as explained in the text. Plot (b) illustrates the relationship between the residual error and the quantity D_t . The solution which has the least residual error is close to the true solution.

FIG. 3. Total magnetic field anomaly in nT in the Arabian Sea from the western continental margin of India. The study area lies to the north of Chagos-Laccadive Ridge system. The estimates of Euler deconvolution are plotted on top of the total magnetic field anomaly. The dashed lines indicate the interpreted basement faults predominantly oriented in the NW-SE and NE-SW directions.

FIG. 4. Histogram of SI obtained from nonlinear optimization of Euler equation assuming nonlinear background. Most of the SI varies between 0.2-0.5 suggesting that the magnetic anomaly is predominantly due to basement faults.

FIG. 5. The solutions of Euler deconvolution are plotted on top of the bathymetry contours from the same region. The sharp basement rise in the center of the grid is due to the associated fracture network. The dashed lines represent the interpreted basement faults predominantly oriented in the NW-SE and NE-SW directions.

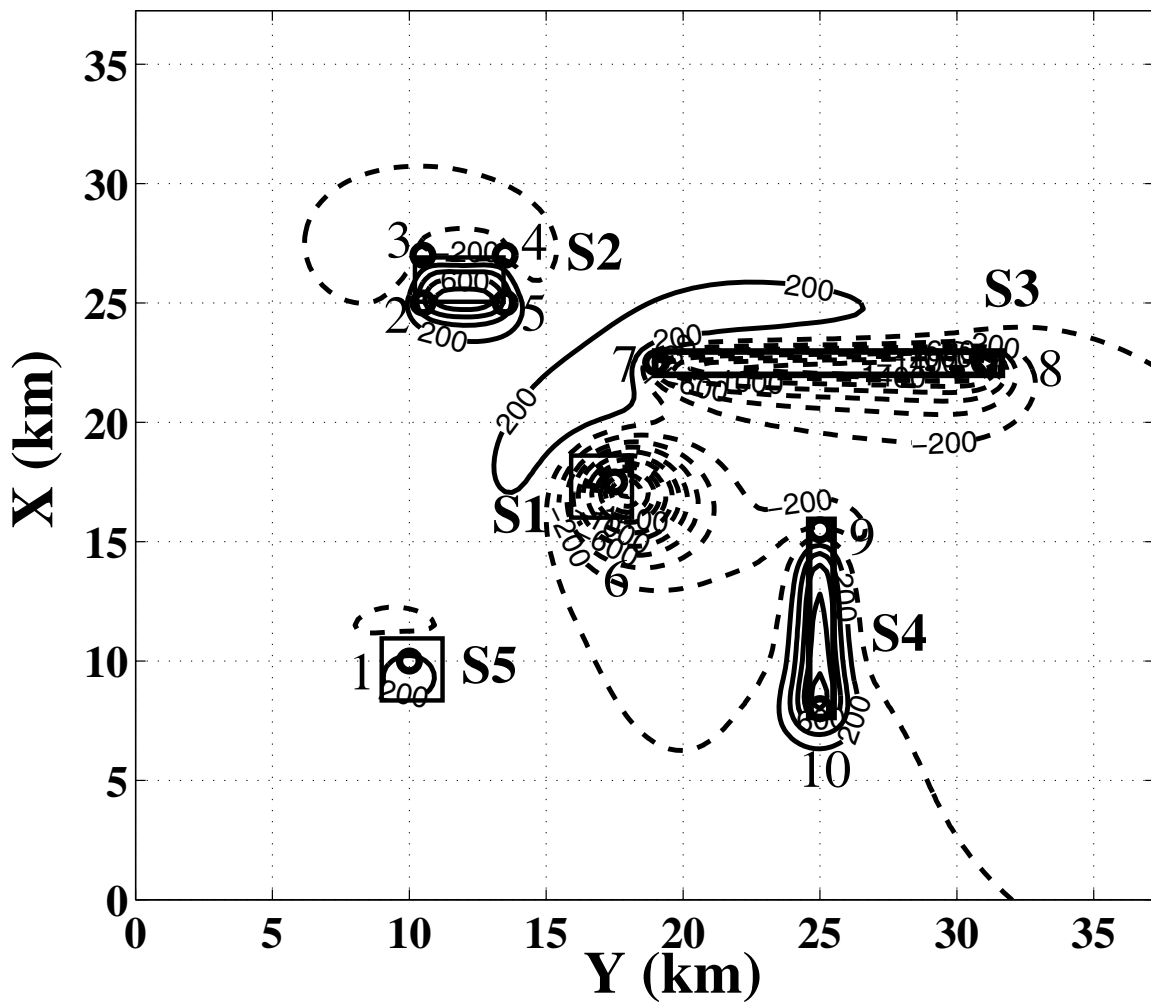


FIG. 1. Total magnetic field anomaly in nT for five simple bodies (after GEROVSKA and ARAÚZO-BRAVO, 2003); S1 and S5 are sphere, S2 is sill body, S3 is a dyke of infinite depth extent, and S4 is a horizontal rod. Each of the singular point is denoted by a circle with a unique number assigned to it.

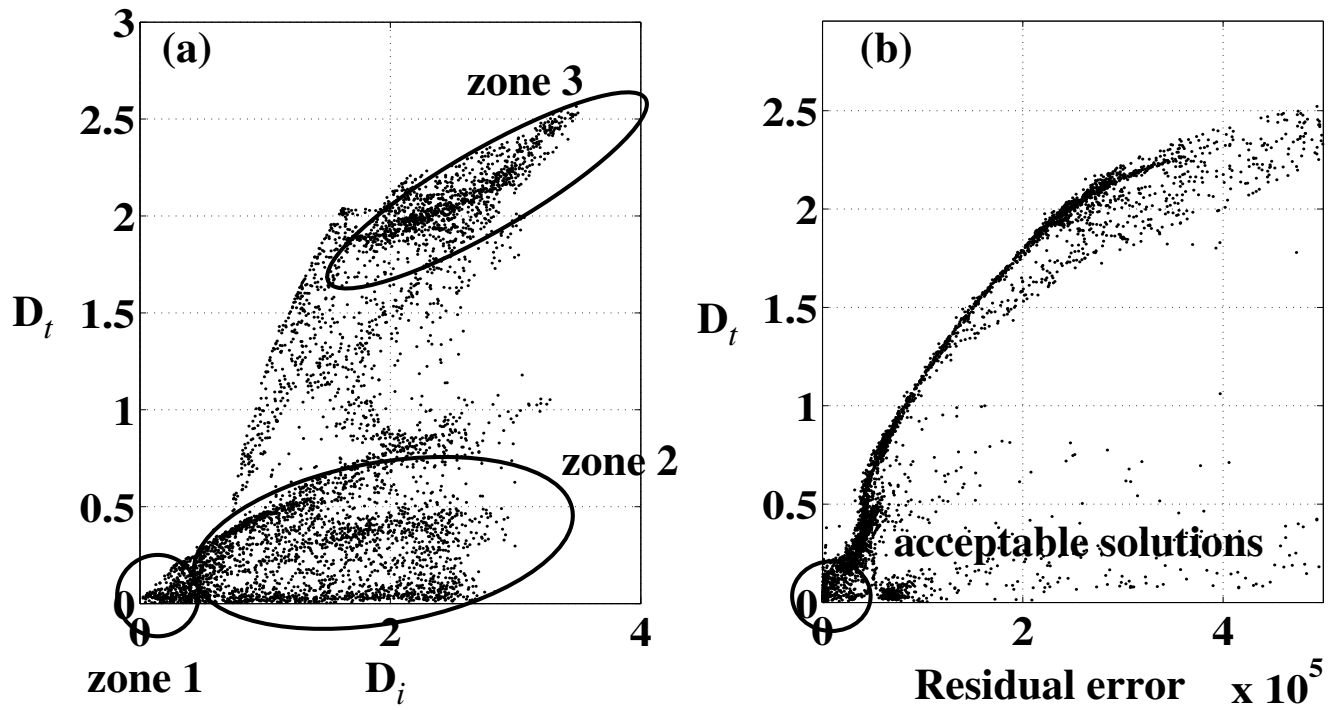


FIG. 2. The performance of the algorithm is evaluated by crossplotting the quantities D_i and D_t as explained in the text. Plot (b) illustrates the relationship between the residual error and the quantity D_t . The solution which has the least residual error is close to the true solution.

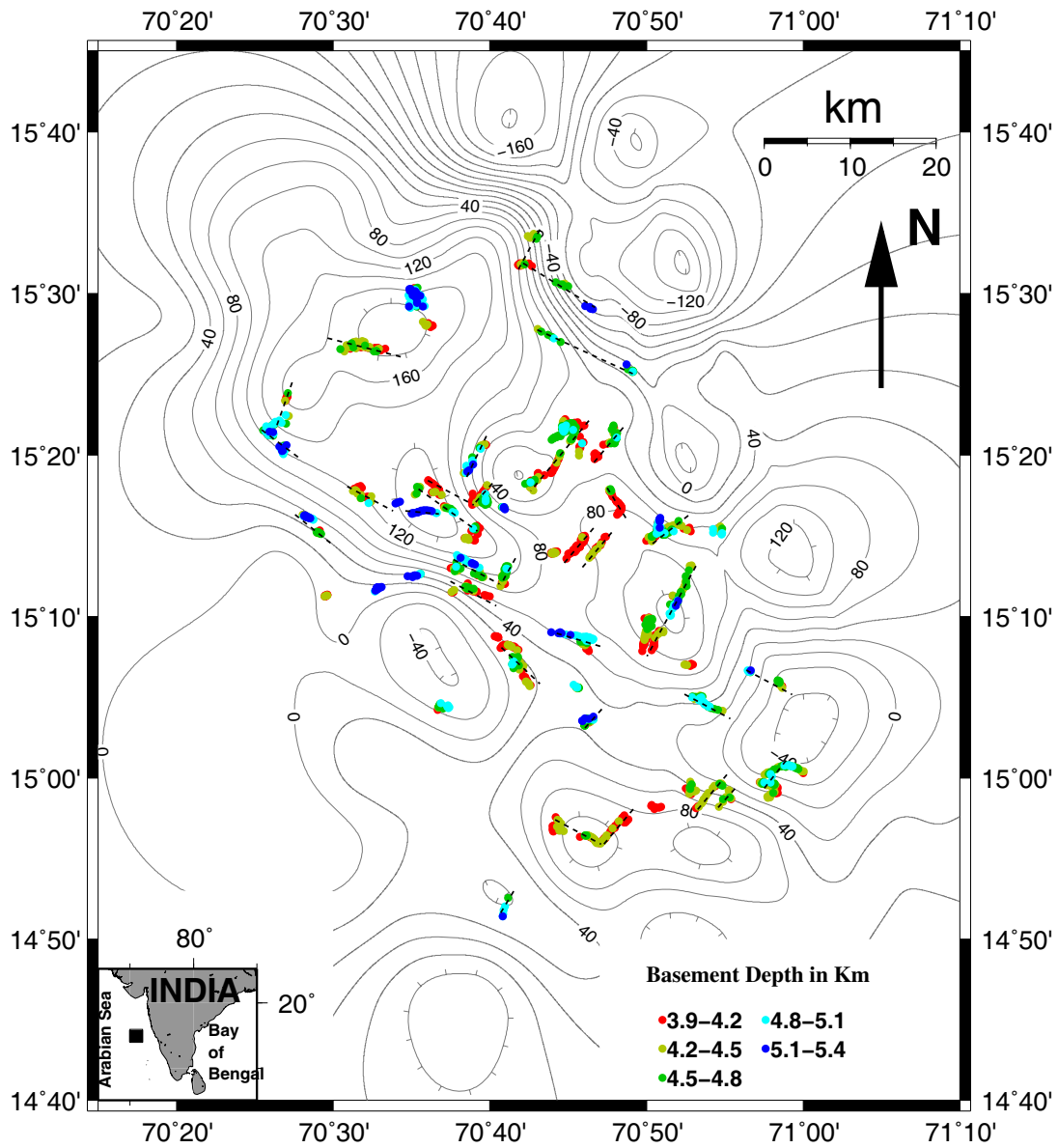


FIG. 3. Total magnetic field anomaly in nT in the Arabian Sea from the western continental margin of India. The study area lies to the north of Chagos-Laccadive Ridge system. The estimates of Euler deconvolution are plotted on top of the total magnetic field anomaly. The dashed lines indicate the interpreted basement faults predominantly oriented in the NW-SE and NE-SW directions.

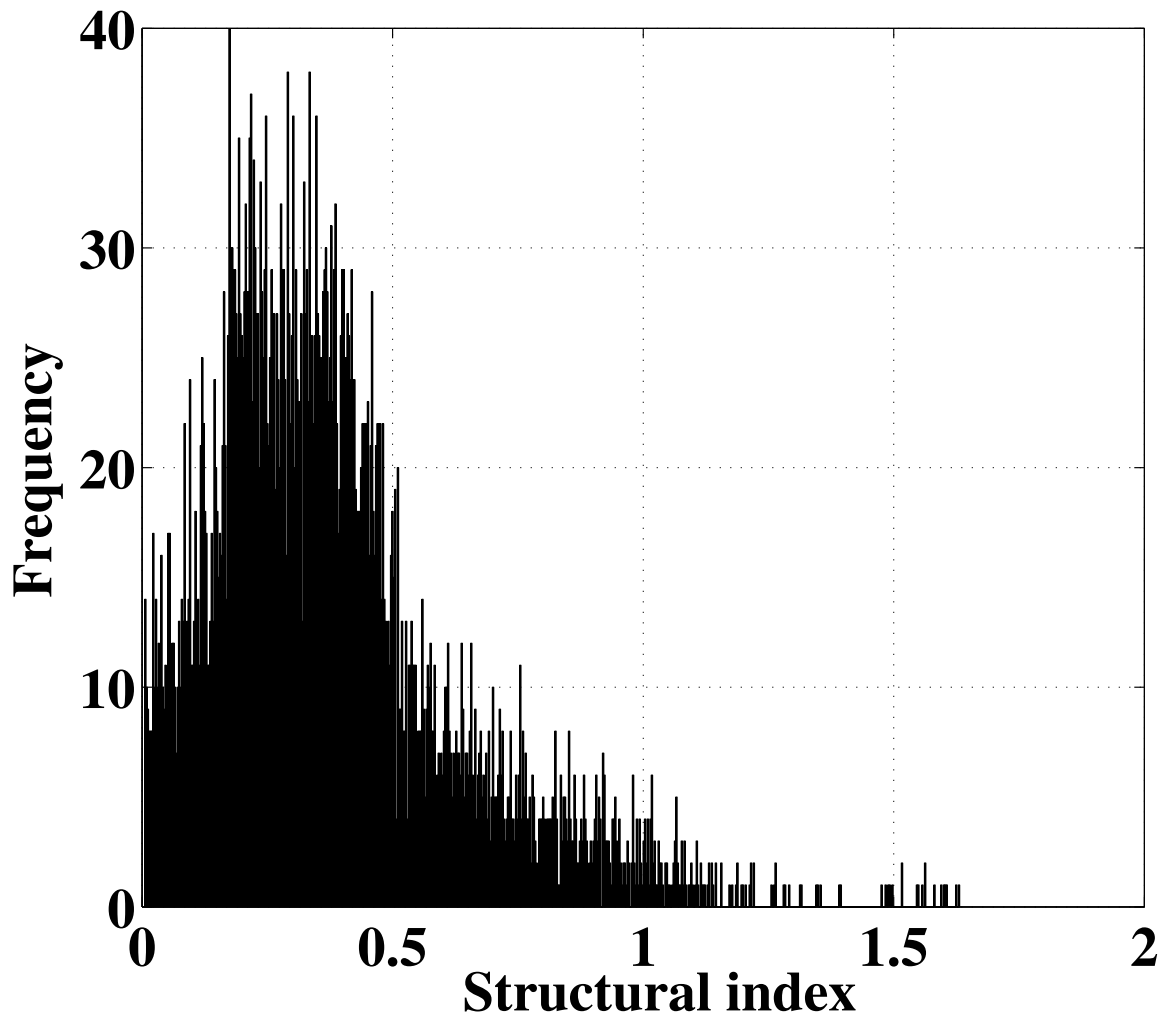


FIG. 4. Histogram of SI obtained from nonlinear optimization of Euler equation assuming nonlinear background. Most of the SI varies between 0.2-0.5 suggesting that the magnetic anomaly is predominantly due to basement faults.

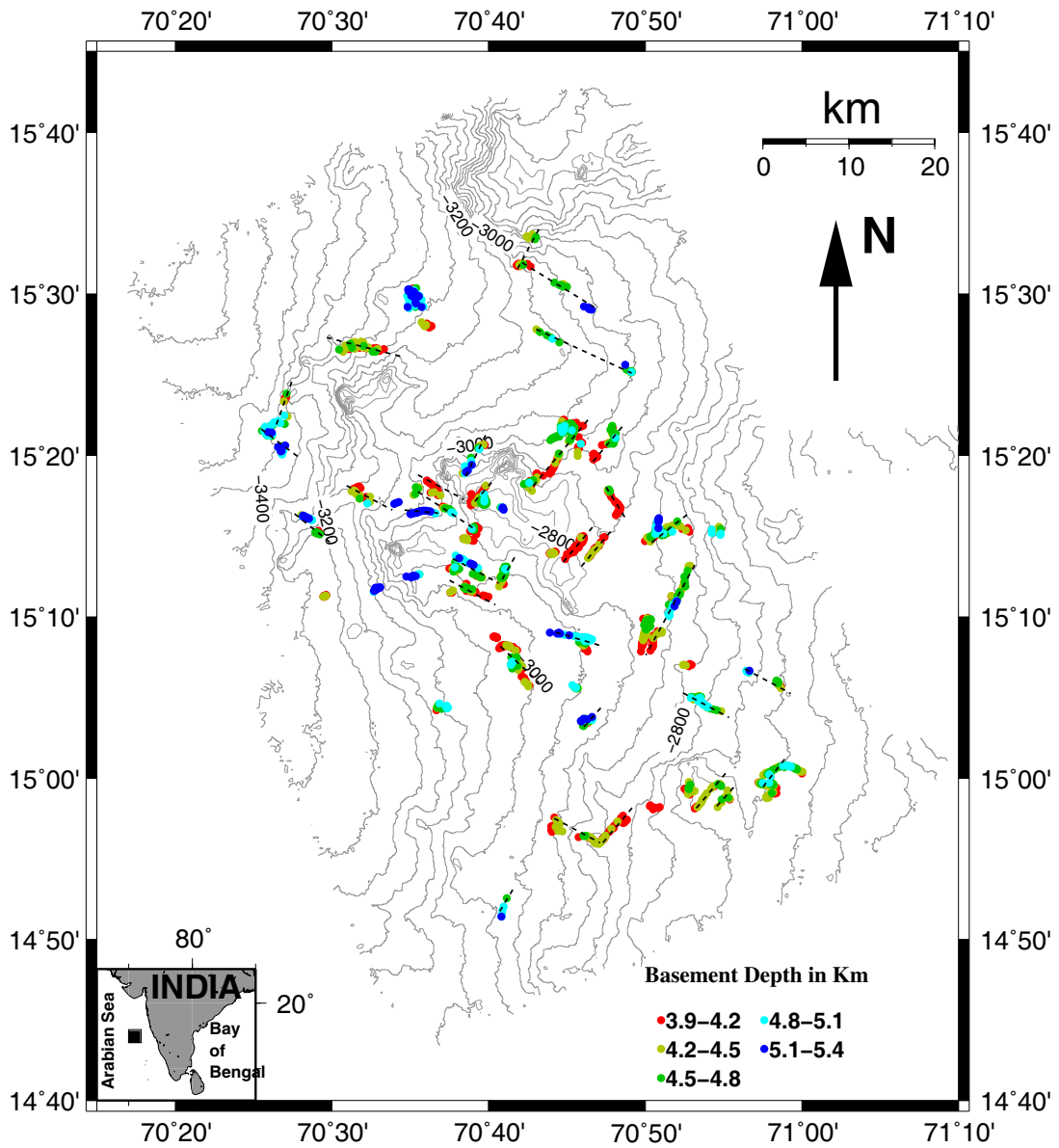


FIG. 5. The solutions of Euler deconvolution are plotted on top of the bathymetry contours from the same region. The sharp basement rise in the center of the grid is due to the associated fracture network. The dashed lines represent the interpreted basement faults predominantly oriented in the NW-SE and NE-SW directions.